nanomaterials

MDPI

Article

Determining the Degree of [001] Preferred Growth of $Ni(OH)_2$ Nanoplates

Taotao Li [1], Ning Dang [2], Wanggang Zhang [1], Wei Liang [1,*] and Fuqian Yang [3,*]

[1] College of Materials Science and Engineering; Shanxi Key Laboratory of Advanced Magnesium-based Materials, Taiyuan University of Technology, Taiyuan, 030024, China; xueyanles10@126.com (T.L.); zwgang0117@163.com (W.Z.)

[2] Laboratoire de Chimie Physique et Microbiologie pour les Matériaux et l'Environnement (LCPME), UMR 7564, CNRS-Université de Lorraine, Villers-lès-Nancy 54600, France; ning.dang@univ-lorraine.fr

[3] Materials Program, Department of Chemical and Materials Engineering, University of Kentucky, Lexington, KY 40506, USA

* Correspondence: liangwei@tyut.edu.cn (W.L.); fyang2@uky.edu (F.Y.)

Received: 13 October 2018; Accepted: 27 November 2018; Published: 30 November 2018

Abstract: Determining the degree of preferred growth of low-dimensional materials is of practical importance for the improvement of the synthesis methods and applications of low-dimensional materials. In this work, three different methods are used to analyze the degree of preferred growth of the $Ni(OH)_2$ nanoplates synthesized without the use of a complex anion. The results suggest that the preferred growth degree of the $Ni(OH)_2$ nanoplates calculated by the March parameter and the expression given by Zolotoyabko, which are based on the analysis and texture refinement of the X-ray diffraction pattern, are in good accordance with the results measured by SEM and TEM imaging. The method using the shape function of crystallites is not suitable for the determination of the preferred growth degree of the $Ni(OH)_2$ nanoplates. The method using the March parameter and the expression given by Zolotoyabko can be extended to the analysis of block materials.

Keywords: degree of preferred growth; $Ni(OH)_2$ nanoplate; shape function

1. Introduction

All polycrystalline materials, including block and powder materials, exhibit preferred orientation of crystallites, to some degree, i.e., texture, due to the mechanical deformation and microstructure evolution during material processing [1–3]. It is of great importance to analyze and determine the preferred orientation when the material properties are orientation-dependent. Electrical, magnetic and mechanical properties of crystals with cubic symmetry are independent on the orientation [4–6].

There are several techniques available to determine the degree of the preferred orientation of powder materials, including optical microscopy (OM), scanning electron microscopy (SEM) and transmission electron microscopy (TEM). The principle in TEM using to determine the preferred growth degree of powder materials is based on the analysis of TEM images and the corresponding diffraction pattern or phase-contrast images along appropriate crystal axis [7]. However, both SEM and TEM can only reveal limited portion of the preferred growth of powder materials, and OM can only be used to analyze the structures with characteristic dimensions more than 200 nm. Also, it is easy to introduce artifacts in replicating real 3-D morphology from projected 2-D images from optical/electronic images, especially TEM images. It is very difficult to use the imaging-related techniques to determine the degree of the preferred growth of nanostructures.

X-ray diffraction (XRD) is another effective way to determine the preferred orientation degree in polycrystalline materials. With a tilting holder in the X-ray diffractometer, pole figure/inverse

pole figure or the orientation distribution function can be used to characterize the blocking materials, such as metals. Yet, there are limited reports on the XRD use in the analysis of the preferred growth degree of powder materials, such as nanostructured $Ni(OH)_2$ and $Cd(OH)_2$ with hexagonal or trigonal symmetry, which have specific preferred growth of [001] [8,9]. In this study, we synthesize $Ni(OH)_2$ nanoplates without the use of any complex anion, and calculate the March parameter (r_n) of the preferred growth with fitting the XRD spectra of the $Ni(OH)_2$ nanoplates by the whole powder pattern fitting method (WPPF) in the framework of the March-Dollase function [10,11]. Afterwards, the degree of the preferred growth degree (η) of the $Ni(OH)_2$ nanoplates is determined with using Zolotoyabko's normalized equation (η_X) [1], the ellipsoidal model (η_E) and direct measurement (η_M) in SEM and TEM images. The preferred growth degree within the ellipsoidal model and direct measurement in SEM and TEM is defined by the ratio of the short axis and long axis in average ($\eta = D_{00l}/D_{hk0}$). The overall aim in this study is to offer a simpler way to determine the degree in the preferred powder materials.

2. Experimental Section

2.1. Fabrication of $Ni(OH)_2$ Nanoplates

$NiCl_2{\cdot}6H_2O$ (99%) and NaOH (99%) were obtained from Sigma-Aldrich (Sinopharm Chemical Reagent Co., Ltd, Shanghai, China) without further purification. The as-received 0.1 M $NiCl_2{\cdot}6H_2O$ of X mL and 0.2 M NaOH of 2X mL were mixed under magnetic stirring to form a homogeneous solution (solvent: deionized water). Multiple centrifugations were used to remove the sodium chloride precipitates from the solution. The homogeneous solution of 40 mL was placed in a Teflon-lined stainless-steel autoclave (Yanzheng experimental instrument co., LTD, Shanghai, China, 60 mL), which was sealed and maintained at 180 °C for 10 h and cooled to room temperature in the furnace. The light green product collected from the Teflon-lined stainless-steel autoclave was washed by distilled water and ethanol. The washed product was dried in a vacuum oven at 60 °C for 6 h.

2.2. Materials Characterization

The XRD analysis of the synthesized products ($Ni(OH)_2$ nanoplates) was performed on a Rigaku X-ray diffractometer (40 kV, 40 mA, Cu Kα radiation: 1.54184 Å, Rigaku Corporation, Akishima-shi, Tokyo, Japan) equipped with a one-dimensional array detector (DteX250(H) Rigaku Corporation, Akishima-shi, Tokyo, Japan) at room temperature. The incident Sola slit and the length of limiting slit are 1/6° and 10 mm, and the scan step is 0.01° for the 2θ in a range of 10° to 100°. The morphology and the electron diffraction pattern of the synthesized products ($Ni(OH)_2$ nanoplates) were analyzed on a scanning electron microscope (MIRA3 LMH, TESCAN Corporation, Brno, Czech) and transmission electron microscope (JEOL 2100F, JEOL ltd, Akishima, Tokyo, Japan), respectively.

2.3. Methodology

The analysis of the XRD patterns was performed, using the software of Rigaku SmartLab Studio II (Rigaku Corporation, Akishima-shi, Tokyo, Japan). The second derivative method was used to identify the diffraction peaks in the XRD patterns, and the split pseudo-Voigt function was used to fit a single peak. The whole powder pattern fitting method (WPPF) without reference to a structural model, as proposed by Pawley in the analysis of the neutron powder data, was used to fit the diffraction spectra [12]. The texture refinement was used to determine the March parameter from the March-Dollase function (W(α)) [10,11]

$$W(\alpha) = \left(r_n^2 \cos^2 \alpha_{n,h} + r_n^{-1} \sin^2 \alpha_{n,h}\right)^{-3/2} \quad (1)$$

here, $\alpha_{n,h}$ is the angle between the orientation vector and diffraction plane vector. The March number r_n determines the preferred orientation strength. The March-Dollase function represents the crystallite fraction with the reciprocal lattice vectors being perpendicular to the sample surface [1]. For $r_n = 1$,

there is no preferred orientation (random orientation); for $r_n < 1$, there is a preferred orientation by plate crystallites with the orientation vector perpendicular to the plate surface; and for $r_n > 1$, there is a preferred orientation by needle crystallites with the orientation vector parallel to the longitudinal direction of needles.

3. Results and Discussion

In Figure 1A, the XRD pattern of the synthesized product is shown, in which all the diffraction peaks can be indexed by the trigonal structure of theophrastite ($Ni(OH)_2$ mineral) with the space group P-3m1 [13]. However, comparing with the peaks calculated from the crystallographic information file (ICSD 24015), as shown by the calculated XRD pattern, a slight offset is observed in the diffraction angles (2θ) between measured data and calculated results, which likely is due to the difference in the lattice constants. After performing the refinement calculation of the lattice constants (a, b and c) and the profile function parameters, we obtain lattice constants of the synthesized $Ni(OH)_2$: a = 3.13212(11) and c = 4.6102(4) Å.

Figure 1A also depicts the calculated XRD pattern of the synthesized $Ni(OH)_2$ with indexed planes. The modified crystallographic file was used in the further profile and texture refinement to determine the preferred direction degree.

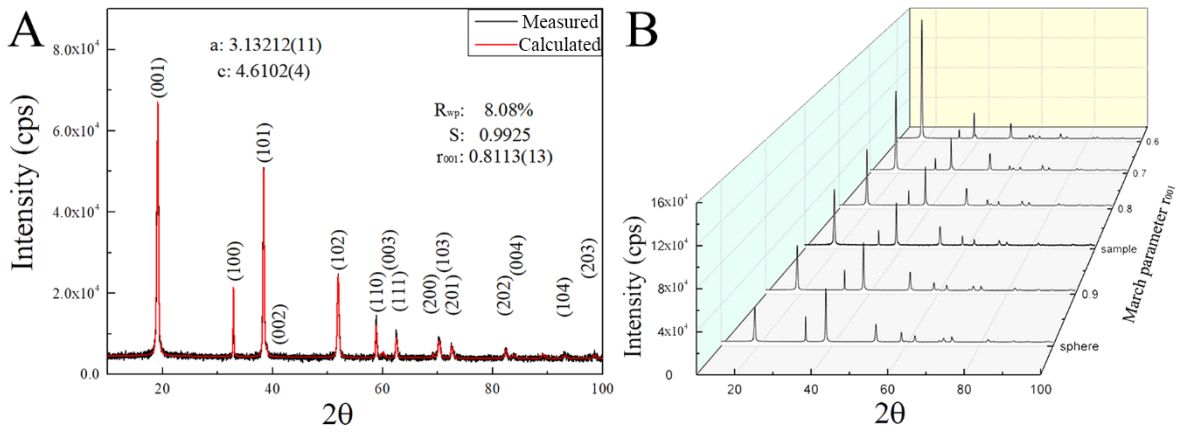

Figure 1. (**A**) The measured and simulated XRD spectra (the smaller the value of R_{wp}, or the closer the value of S to 1, the better is the match between the measured and simulated data), and (**B**) the simulated XRD diffraction spectra with strong preferred orientation of the [001] type ($r_n = 1$ (sphere) without preferred orientation; $r_n < 1$ with the preferred orientation by plate crystallites; and $r_n > 1$ with the preferred orientation by needle crystallites).

Table 1. FWHM (β) of the measured peaks of $Ni(OH)_2$ after the correction of the instrumental broadening by external standard method (Si) from Rigaku.

2θ (°)	Int. W (°)	hkl	2θ (°)	Int. W (°)	hkl
19.147	0.395	001	69.201	0.09	200
32.877	0.083	100	70.24	0.53	103
38.380	0.235	101	72.545	0.40	201
38.92	0.54	002	82.43	0.38	202
51.920	0.38	102	83.91	0.33	004
58.860	0.143	110	93.10	0.46	104
60.22	0.43	003	98.45	0.42	203
62.529	0.22	111			

It is known that diffraction peak experiences an angle broadening in crystalline materials with grain size less than 100 nm or under lattice strain [14]. The diffraction peak broadening for the synthesized $Ni(OH)_2$ is likely due to the submicron crystallite sizes. From Figure 1A, we note that

the FWHM (full width at half maximum) of the (001) diffraction peak of $Ni(OH)_2$ is much wider than those of (100) and (110), suggesting that the crystallite size along the [001] direction is much smaller than those along the [100] and [110] directions and the crystallites of $Ni(OH)_2$ are ellipsoidal instead of spherical shape.

To separate the instrumental broadening from the peak broadening of $Ni(OH)_2$, we used a silicon standard specimen for the instrumental broadening estimation during the comprehensive analysis of the synthesized $Ni(OH)_2$ by SmartLab Studio II. Table 1 lists the corrected FWHM values of the synthesized $Ni(OH)_2$. The FWHM of the peaks (001), (002), (003) and (004) are 0.395, 0.54, 0.43 and 0.33°, respectively, which are much larger than those of the other peaks; the FWHM of the peaks (100), (110) and (200) are 0.083, 0.143 and 0.09°, respectively. The analysis of the widest peak (00l) and the narrowest peak (hk0) parameters suggests that the synthesized $Ni(OH)_2$ crystallites are two-dimensional in shape, and the diameter of synthesized $Ni(OH)_2$ crystallites along [hk0], D_{hk0}, is much larger than that along the [00l] direction, D_{00l}. Thus, the synthesized $Ni(OH)_2$ is present in the two-dimension nanoplate shapes.

In the standard diffraction spectra calculated with spherical crystallites, the integrated intensity of (101) should be larger than that of (001), as shown in Figure 1B (sphere). According to the measured diffraction data, there exists the preferred growth of $Ni(OH)_2$ crystallites responsible for the abnormal integrated intensity ratio between (001) and (101). Using the March-Dollase function in the smartLab Studio II, we performed the profile and texture refinement to determine the degree of the preferred direction [001], i.e., the smallest dimension of the two-dimensional $Ni(OH)_2$ crystallites. The calculation gives the March parameter of $r_{001} = 0.8113$, as shown in the calculated XRD spectrum of Figure 1A with $R_{wp} = 8.08\%$ and $S = 0.9925$.

Figure 1B depicts the variation of the simulated diffraction spectra with the March parameter r_{00l}. Increasing the March parameter r_{00l} leads to the increase of the intensity ratio between (001) and (101). This ratio likely represents the preferred growth degree of the synthesized $Ni(OH)_2$. The standard theophrastite (JCPDS. No.14-0117) given by ICDD also shows preferred growth because the ratio of the diffraction intensity of (001) and (101) is 1. Yet, the March parameter r_{00l} cannot effectively represent the preferred growth degree of the 2-D $Ni(OH)_2$ crystallites.

Zolotoyabko established a relationship between the degree of preferred growth and the March parameter r_n extracted from diffraction measurements using the nominalized March-Dollase function $W(\alpha)$. He proposed that the degree of preferred growth can be expressed by η as

$$\eta = 100\% \left[\frac{(1 - r_n)^3}{1 - r_n^3} \right]^{1/2} \quad (2)$$

for $r_{001} = 0.8113$, we obtain the degree of the [001] preferred growth deduced in X-ray diffraction, η_X, as 12.00%.

Žunić and Dohrup demonstrated that an ellipsoid in reference to crystallographic axes (triclinic case) can be expressed as [15]

$$b_{11}x_c^2 + b_{22}y_c^2 + b_{33}z_x^2 + 2b_{12}x_cy_c + 2b_{13}x_cz_c + 2b_{23}y_cz_c = 1 \quad (3)$$

where b_{ij} (i, j = 1, 2, 3) are the coefficients related to reciprocal axes. The symbols x_c, y_c and z_c stand for the parameters in describing the surface function. Thus, the simulated ellipsoid can be expressed as

$$b_{11}h^2 + b_{22}k^2 + b_{33}l^2 + 2b_{12}hk + 2b_{13}hl + 2b_{23}kl = \frac{9}{16D_{hkl}^2 d_{hkl}^2} \quad (4)$$

here, D_{hkl} is the surface average diameter of the ellipsoidal crystallites (D_{00l} and D_{hk0}) obtained from the normalized expressions of anisotropic line broadening, and d_{hkl} is the interplanar spacing. The meanings of the letters: h, k and l are consistent with the subscript in D_{hkl} and d_{hkl}. Table 2 lists

the coefficients of the refined ellipsoidal crystallites of the synthesized $Ni(OH)_2$. Using the fitting coefficients for the synthesized $Ni(OH)_2$, we obtain the main diameters of D_{00l} and D_{hk0} as 31.40 and 185.95 nm, respectively. The synthesized $Ni(OH)_2$ indeed is present in the shape of nanoplates with the [001] preferred growth and the degree (η_E) of the [001] preferred growth is 16.89%.

Table 2. Coefficients of the ellipsoid in simulating the preferred growth of $Ni(OH)_2$ (the ellipsoid is characterized by six coefficients).

b_{11}	b_{22}	b_{33}	b_{12}	b_{13}	b_{23}
7.029E-8	7.029E-8	8.506E-7	3.515E-8	0	0

Figure 2A,B,D,E shows the SEM and TEM images of the synthesized $Ni(OH)_2$, confirming the shape of nanoplates determined by the analysis of the XRD pattern via the whole powder pattern. Figure 2C depicts the selected area electron diffraction (SAED) pattern of the $Ni(OH)_2$ nanoplates. If the diameter of a grain in the preferred direction is much longer or shorter than that of its normal directions, it can be rendered as the preferred growth. Thus, the $Ni(OH)_2$ nanoplates exhibit six-fold symmetry about the [001] direction in accordance with the preferred growth obtained by X-ray diffraction. The synthesized $Ni(OH)_2$ powder contains two-dimension nanoplates with the normal of the surface of the nanoplates being (001) and D_{00l} being much smaller than D_{hk0}. To confirm the trigonal symmetry, in Figure 2C, the SAED pattern is shown for a single crystal $Ni(OH)_2$ nanoplate. Thus, the degree of the preferred growth of $Ni(OH)_2$ grains characterized by the X-ray diffraction could be revealed by the $Ni(OH)_2$ nanoplates observation by SEM and TEM. It needs to point out that the phase-contrast images may not reveal the structure of the $Ni(OH)_2$ nanoplates due to possible damage induced by electron beam with an energy of 200 KeV.

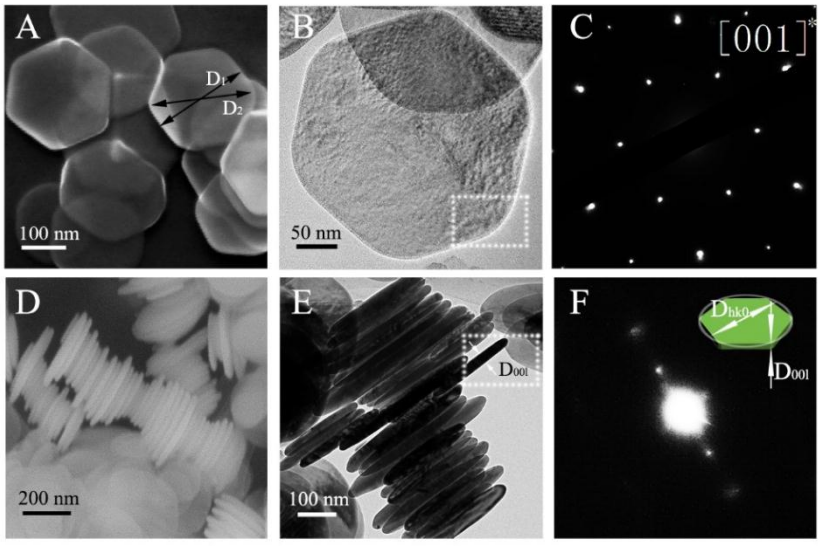

Figure 2. (**A**) SEM and (**B**) TEM images of $Ni(OH)_2$ nanoplates (top view), (**C**) SAED pattern of the square area in B, (**D**) SEM and (**E**) TEM mages of $Ni(OH)_2$ nanoplates (side view), and (**F**) SAED pattern of the square area in E (The inset in F is a schematic of a $Ni(OH)_2$ nanoplate showing the diameter of D_{hk0} and D_{00l}).

Figure 2D,E shows the SEM and TEM images of the side surfaces of the synthesized $Ni(OH)_2$ nanoplates. The SAED pattern of the square area in Figure 2E is shown in Figure 2F. The one-way diffraction spots revel the spacing of [001] for the $Ni(OH)_2$ nanoplates in consistence with the plane (001) normal of the surface of the nanoplates. Note that the crystal orientation cannot be indexed by the one-way diffraction pattern.

With using an ellipsoid model, Žunić and Dohrup proved that the average ellipsoid size follows an equivalent ellipsoidal function in X-ray diffraction [15]. As follows from Equation 1, the orientation distribution depends only on March parameter (r) and angle (θ), with no crystallite size being involved. However, the degree of the preferred $Ni(OH)_2$ nanoplates could be determined from measuring the edge length of the preferred growth and its normal diameter. Thus, the preferred direction and normal direction diameters are measured to confirm the results in X-ray diffraction. In this paper, the degree of averaged crystallite shape in [001] preferred $Ni(OH)_2$ is simply defined as the ratio of D_{00l} and D_{hk0} labelled in Figure 2F. From Figure 2D,E, we note that there are some $Ni(OH)_2$ nanoplates tilted or truncated, and expect to obtain a distribution of the diameters of D_{hk0} and D_{00l}. Statistical analysis of the SEM and TEM images of the side surfaces of 288 $Ni(OH)_2$ nanoplates was performed in Image J to calculate the diameters of D_{hk0} and D_{00l}. We obtain D_{00l} of 24.34 ± 3.54 nm.

Figure 3 shows the distribution of D_{hk0} of the $Ni(OH)_2$ nanoplates over 288 nanoplates. The D_{hk0} is in the range of 129.31–539.68 nm, and the averaged D_{hk0} is 278.4 nm. Using the D_{hk0} and D_{00l}, we obtain the degree of [001] preferred growth as 8.74%. The λ-like distribution of the D_{hk0} of the $Ni(OH)_2$ nanoplates, as shown in Figure 3, reveals the difficulty in the counting of $Ni(OH)_2$ nanoplates of small diameters, resulting in smaller η_M than η_X. We conclude that the degree of the [001] preferred growth of the $Ni(OH)_2$ nanoplates, η_X, calculated by the WPPF reflects the degree of the [001] preferred growth of the $Ni(OH)_2$ nanoplates, η_M.

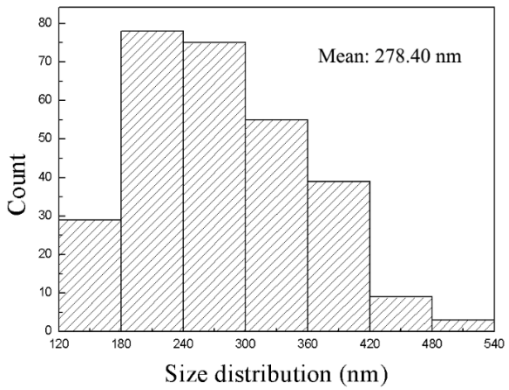

Figure 3. Distribution of D_{hk0} of the $Ni(OH)_2$ nanoplates over 288 nanoplates.

Compared the values of 278.40 and 24.34 nm of D_{hk0} and D_{00l} measured by SEM and TEM with those of 185.95 and 31.40 nm calculated from the ellipsoidal model, we note that there are significant differences between the corresponding values. The shape function of crystallites is not suitable for the description of the shape of nanoplates, and the calculated values cannot be used to represent diameters of D_{hk0} and D_{00l} of the $Ni(OH)_2$ nanoplates.

For the situation when the shape parameters of crystallites cannot be accounted for the actual sizes, an average spherical shape can be assumed. Using the Halder-Wagner's method, we can calculate D_{hk0} from the slope of the line plotting of $\beta^2 / \tan^2\theta$ vs. $\beta / \tan\theta \sin\theta$ for the FWHM of (100), (110)and (200) and D_{00l} from the FWHM of (001), (002), (003) and (004) [16]. As shown in Figure S1 the calculated diameters of D_{00l} and D_{hk0} are 22.2 ± 1.3 and 93.7 ± 14.1 nm, respectively. The edge length in [001] of the $Ni(OH)_2$ is in good relation to the results 24.34 nm determined by SEM and TEM images. The diameter of the crystallites below 100 nm will result the widening in the diffraction peaks, which may be accounted for the inappropriate edge length in [hk0] [14].

4. Summary

We have synthesized $Ni(OH)_2$ nanoplates without the use of any complex anion. Three different methods are used to analyze the degree of preferred growth of the $Ni(OH)_2$ nanoplates. Using the March-Dollase method and the whole powder pattern fitting method, we obtain the March parameter of r_{00l} = 0.8113 through the texture refinement. The degree of [001] preferred growth of the $Ni(OH)_2$

nanoplates, η_X, is found to be 12.00% from the March parameter of r_{001} and the normalized expression given by Zolotoyabko. The shape function of crystallites is not suitable to directly describe the shape of the $Ni(OH)_2$ nanoplates. Using the Halder-Wagner's method, we obtain the edge length of D_{001} as 22.2 ± 1.3 nm that is in good relation to the results measured by SEM and TEM imaging. The TEM imaging of the $Ni(OH)_2$ nanoplate reveals that the $Ni(OH)_2$ nanoplates exhibit six-fold symmetry about the [001] being the preferred growth. The measured degree of [001] preferred growth of the $Ni(OH)_2$ nanoplates, η_M, is 8.74%, slightly less than η_X. The March parameter and the expression given by Zolotoyabko can be used to effectively calculate the degree of preferred growth of nanostructural materials ($0 < r < 1$), which can be extended to the analysis of block materials.

Supplementary Materials: The following are available online at http://www.mdpi.com/2079-4991/8/12/991/s1, Figure S1: The simulated linear function with Halder-Wagner's method. The Diameters of D_{001} and D_{hk0} are determined.

Author Contributions: Taotao Li, conceptualization, methodology, software and writing-original draft preparation. Wanggang zhang and Fuqian yang, writing-review & editing and visualization. Funding Acquisition, Pro. Wei Liang. Ning Dang, discussion on the preferred orientation and preferred growth.

Funding: This work was supported by the National Natural Science Foundation of China (No. 51274149, NO. 51175363 and NO. 51474152) and Projects of International Cooperation in Shanxi, No.:201603D421026.

Acknowledgments: I am much indebted to Dr. Huihu Lu in Taiyuan University of Technology for his kind interest and supervision.

Conflicts of Interest: The authors declare no conflict of interest.

References

1. Zolotoyabko, E. Determination of the degree of preferred orientation within the March-Dollase approach. *J. Appl. Crystallogr.* **2009**, *42*, 513–518. [CrossRef]
2. Atuchin, V.V.; Chimitova, O.D.; Gavrilova, T.A.; Molokeev, M.S.; Kim, S.J.; Surovtsev, N.V.; Bazarov, B.G. Synthesis, structural and vibrational properties of microcrystalline RbNd(MoO4)2. *J. Cryst. Growth* **2011**, *318*, 683–686. [CrossRef]
3. Atuchin, V.V.; Beisel, N.F.; Kokh, K.A.; Kruchinin, V.N.; Korolkov, I.V.; Pokrovsky, L.D.; Tsygankova, A.R.; Kokh, A.E. Growth and microstructure of heterogeneous crystal GaSe:InS. *Crystengcomm* **2013**, *15*, 1365–1369. [CrossRef]
4. Li, B.L.; Godfrey, A.; Meng, Q.C.; Liu, Q.; Hansen, N. Microstructural evolution of IF-steel during cold rolling. *Acta Mater.* **2004**, *52*, 1069–1081. [CrossRef]
5. Liu, H.; Liu, Z.; Cao, G.; Li, C.; Wang, G. Microstructure and texture evolution of strip casting 3 wt% Si non-oriented silicon steel with columnar structure. *J. Magn. Magn. Mater.* **2011**, *323*, 2648–2651. [CrossRef]
6. Song, H.Y.; Liu, H.T.; Lu, H.H.; An, L.Z.; Zhang, B.G.; Liu, W.Q.; Cao, G.M.; Li, C.G.; Liu, Z.Y.; Wang, G.D. Fabrication of grain-oriented silicon steel by a novel way: Strip casting process. *Mat. Lett.* **2014**, *137*, 475–478. [CrossRef]
7. Li, T.; Dang, N.; Liang, M.; Guo, C.; Lu, H.; Ma, J.; Liang, W. TEM observation of general growth behavior for silver electroplating on copper rod. *Appl. Surf. Sci.* **2018**, *451*, 148–154. [CrossRef]
8. Mao, Y.; Li, T.; Guo, C.; Zhu, F.; Zhang, C.; Wei, Y.; Hou, L. Cycling stability of ultrafine β-$Ni(OH)_2$ nanosheets for high capacity energy storage device via a multilayer nickel foam electrode. *Electrochim. Acta* **2016**, *211*, 44–51. [CrossRef]
9. Ghoshal, T.; Kar, S.; Chaudhuri, S. Synthesis of nano and micro crystals of $Cd(OH)_2$ and CdO in the shape of hexagonal sheets and rods. *Appl. Surf. Sci.* **2007**, *253*, 7578–7584. [CrossRef]
10. March, A. Mathematische Theorie der Regelung nach der Korngestah bei affiner Deformation. *Z. Krist.-Cryst. Mater.* **1932**, *81*, 285–297. [CrossRef]
11. Dollase, W.A. Correction of intensities for preferred orientation in powder diffractometry: Application of the March model. *J. Appl. Crystallogr.* **1986**, *19*, 267–272. [CrossRef]
12. Pawley, G.S. Unit-cell refinement from powder diffraction scans. *J. Appl. Crystallogr.* **1981**, *14*, 357–361. [CrossRef]

13. Cairns, R.W.; Ott, E. X-Ray Studies of the System Nickel-Oxygen-Water. I. Nickelous Oxide and Hydroxide1. *J. Am. Chem. Soc.* **1933**, *55*, 527–533. [CrossRef]
14. Langford, J.I.; Wilson, A.J.C. Scherrer after sixty years: A survey and some new results in the determination of crystallite size. *J. Appl. Crystallogr.* **1978**, *11*, 102–113. [CrossRef]
15. Balić Žunić, T.; Dohrup, J. Use of an ellipsoid model for the determination of average crystallite shape and size in polycrystalline samples. *Powder Diffr.* **1999**, *14*, 203–207. [CrossRef]
16. Halder, N.C.; Wagner, C.N.J. Separation of particle size and lattice strain in integral breadth measurements. *Acta Crystallogr.* **1966**, *20*, 312–313. [CrossRef]